

## An Anisotropic Ink Based on Crystalline Nanocellulose: Potential Applications in Security Printing

Chakkresit Chindawong, Diethelm Johannsmann

Institute of Physical Chemistry, Clausthal University of Technology, 38678 Clausthal-Zellerfeld, Germany

Correspondence to: D. Johannsmann (E-mail: johannsmann@pc.tu-clausthal.de)

**ABSTRACT:** Polymer dispersions containing crystalline nanocellulose have been used as birefringent inks. When printed onto dark paper, the letters are darker than the background if viewed without polarizers, while they are brighter than the background if viewed with crossed polarizers. This type of contrast inversion can have applications in security printing and optical authentication. © 2014 Wiley Periodicals, Inc. *J. Appl. Polym. Sci.* **2014**, *131*, 41063.

**KEYWORDS:** cellulose and other wood products; coatings; colloids; latices; optical properties

Received 17 April 2014; accepted 23 May 2014

DOI: 10.1002/app.41063

### INTRODUCTION

Security printing relies on patterns, which are easily recognized, on the one hand, but are not easily forged, on the other.<sup>1</sup> As recognition occurs by visual inspection, security printing often exploits features with a peculiar optical appearance. Examples are holograms, colored fibers, and watermarks. Intricate schemes of printing play a role, but particular types of inks (often combined with certain printing procedures) are used, as well. Such inks can make use of fluorescence,<sup>2</sup> up-conversion from the infrared, or opalescence (also called “iridescence”).<sup>3</sup> The latter effect relies on interference. The resulting colors are impressive and, also, change with the angle of observation. A second class of optically variable inks (OVI's) relies on reflective pigment particles with platelet-shape.<sup>1</sup> If the platelets have a preferred orientation, their appearance depends on the angle of observation.

Birefringence is known to produce a variety of interesting optical effects (including angle-dependent colors), when the object of interest is placed between crossed polarizers and viewed in transmission. However, a peculiar appearance must be obtained in reflection (diffuse or specular), if it shall be of use in security printing. This entails a difficulty in so far, as the diffuse and depolarized reflection from a white background can easily mask all effects of polarization. White paper reflects light randomly, which implies that the polarization of the reflected photons is largely uncorrelated to the incident polarization. The depolarization is a consequence of multiple scattering. Many inks are similar to paper in this regard. They differ from the background in their color, but conventional inks are designed to be strong scatterers just like the paper itself, which entails multiple scattering.

This behavior contrasts to the behavior of translucent, birefringent ink, for instance composed of crystalline nanocellulose (CNC). CNC layers scatter light only weakly. Because single scattering dominates, the polarization is preserved to a certain extent<sup>4</sup> and polarization effects can be observed even in diffuse reflection. However, the scattered intensity from the ink cannot be seen against an unpolarized background, if the latter is white paper. A white background spoils all polarization effects.

These problems can be overcome by applying the CNC-based ink to dark paper. With a dark background, multiple scattering is reduced to the extent that the diffuse reflectance is attenuated by a factor of 2–3 under crossed polarizers (see, for instance, Figure 4). The preservation of polarization is the consequence of single scattering.<sup>4</sup>

Figure 1 demonstrates the effect. The letter “A” was written with pure nanocellulose (left), with a blend of nanocellulose and a polymer latex (center), and with a latex dispersion containing no nanocellulose (right). The different images were taken with parallel polarizers (A), crossed polarizers (B), and without polarizers (D). There is contrast inversion between panels A and B. Panel C shows a spin-cast CNC film imaged with crossed polarizers as in panel B. Spin-casting orients the CNC layer, where the rods line up along the radial direction. Areas, inside which the rods make an angle with the polarizers, appear bright (for similar reasons as in transmission). Panels B and D (“crossed polarizers” and “no polarizers”) also differ in appearance, but the effects are less impressive than the comparison between panels A and B. If parallel and crossed polarizers cannot both be afforded, instrumentally, the comparison between “crossed polarizers” and “no polarizers” will still yield an effect.

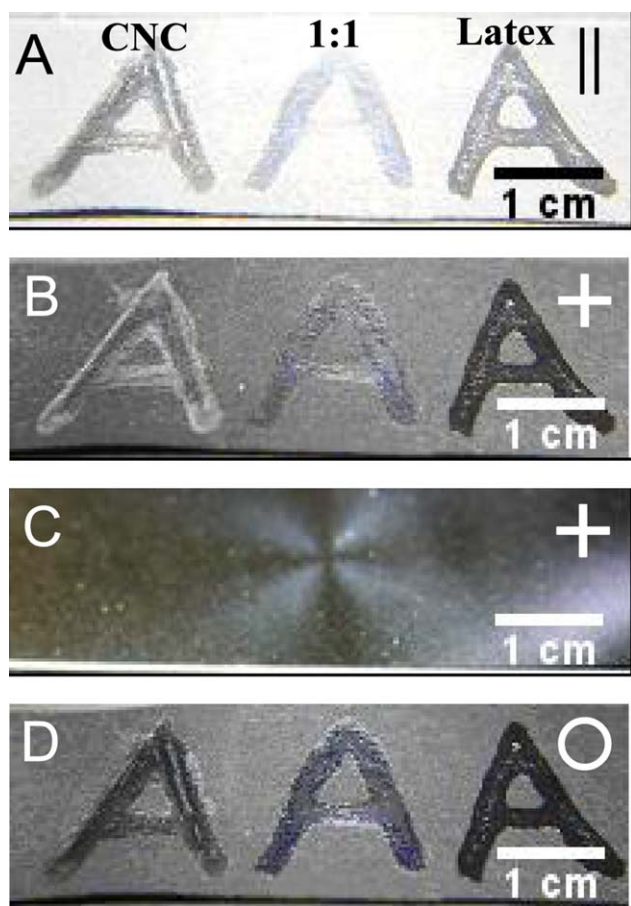


**Figure 1.** The letter “A” was written onto black paper with pure nanocellulose (left), a blend of nanocellulose with a latex dispersion (center), and a pure latex dispersion (right). The images in panels A, B, and D were acquired with parallel polarizers, with crossed polarizers, and without polarizers, respectively. Panel C shows a spin-cast film of nanocellulose imaged under same conditions as in panel B. Spin-casting leads to highly oriented films. One observes a Maltese cross in Panel C, where the center of the cross is the rotation axis during spin casting. For the inks containing nanocellulose, there is contrast inversion between panels A and B. For the arrangement of the sample, the light source, the camera, and the polarizers see Figure 3. [Color figure can be viewed in the online issue, which is available at [wileyonlinelibrary.com](http://wileyonlinelibrary.com).]

The comparison between parallel and crossed polarizers (panels A and B) still is the first choice for easy visual discrimination. Figure 1 was acquired in the laboratory with polarizers mounted in front of the light source and the camera. However, devices visualizing polarization effects can be simpler than that. Figure 2 shows a sketch of a flash lamp with a polarizer glued to the front of the LED and a second polarizer attached to its side. Such a device can be cheap; its application is trivial.

CNC has been known since the early 1950s.<sup>5</sup> Its availability has improved recently, which has led to a surge in interest. Among the benefits of cellulose as a material is its origin from natural resources. Overviews over the properties and the applications of nanocellulose can be found in Refs. 6–8. The focus in this work is on the optical properties of dried nanocellulose and on

potential applications in optics. The material used (supplied by the Forest Products Laboratory, Madison, WI), is composed of nanorods with a diameter of 5 nm and a length in the range between 100 and 200 nm.<sup>9</sup> Dispersions in water are isotropic at concentrations below 5% and form a chiral-nematic phase at concentrations larger than 15%. There is phase coexistence between 5% and 15%. The dried material forms a glassy phase with a smooth surface.<sup>10,11</sup>

Because the rods giving rise to liquid crystalline behavior are of colloidal dimensions, it is easy to produce alignment. Put differently, some kind of alignment actually cannot be avoided during application of the ink because the spreading process is accompanied by shear flow. Droplets applied by inkjet printing are birefringent. The pattern of orientation reflects the flow during deposition.<sup>12</sup> If good alignment is required, one can shear the material after deposition with a doctor blade as demonstrated in Refs. 13,14.

While birefringence and even intricate patterns of birefringence are easily obtained, it is difficult to achieve clear films for a number of reasons. Because cellulose is chiral, CNC dispersions (and also the dried films) have a tendency to develop twist. When blending nanocellulose with a polymer dispersion and shearing the material, one can overcome the twist and achieve uniaxial anisotropy, but these films still show a texture under the microscope. The texture may be caused by orientation fluctuations, concentration fluctuations, or packing defects. Packing imperfections can give rise to interesting super-structures as proposed in Ref. 15. Still, they amount to a problem in those applications, where clarity is required. Evidently, this includes a large number of potential uses of CNC in optics. Security printing in this regard is special. The application of nanocellulose as an ink does not require optical clarity. On the contrary, a small amount of turbidity helps to recognize the material as being special.

Security printing applications of nanocellulose have been proposed before.<sup>16,17</sup> Gray and co-workers have shown that nanocellulose dispersions can be dried in such a way that the material’s chirality is preserved and that the pitch is in the range of the wavelength of light. The material then produces iridescent colors.<sup>18</sup> The effects discussed below are *not* based on chirality but on nematic order. We did observe a slight bluish coloration, occasionally, but we do not exploit it. Most of the time, the pitch was too long to generate interference colors. Chirality can still be useful for inks, in principle, because chirality induces a specific texture. Texture is not the focus of the work reported here.

Dispersions of nanocellulose are not practical inks because the dried material can be redispersed in water. However, a water-proof material with similar properties is obtained by blending the nanocellulose with a latex dispersion. Such blends have been studied before in the context of mechanical reinforcement.<sup>19–21</sup> A blend of an acrylic latex with a glass transition temperature,  $T_g$ , of 4°C and a CNC dispersion was employed here. We will report on the film formation properties of CNC/

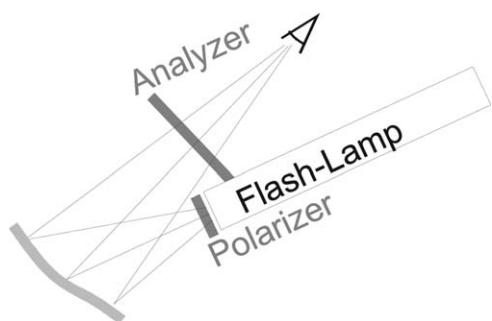


**Figure 2.** A simple testing device for polarizing inks.

latex blend separately. This work concerns the application as an ink.

## EXPERIMENTAL

The crystalline nanocellulose employed was produced by the Forest Products Laboratory (FPL, Madison, WI) and purchased through the University of Maine.<sup>22</sup> Details on the production process and on material properties are provided on the homepage of the University of Maine.<sup>9</sup> The nanocellulose was delivered in powder form and dispersed in water by sonication.

Latex dispersions were prepared by miniemulsion polymerization. The monomers were methylmethacrylate (MMA, Carl Roth, 99%, 49.5 wt %), *n*-butylacrylate (BA, Aldrich, 99%, 49.5 wt %), and acrylic acid (AA, Fluka, 99%, 1.4 wt %). The composition of the copolymer was 49.5/49.5/1 wt % MMA/BA/AA. Sodium dodecyl sulfate (SDS, Carl Roth, 99%, 2 wt %) was used as surfactant, hexadecane (HD, Aldrich, 99%, 3.7 wt %) was used as the co-stabilizer, and azo-*bis*-isobutyronitrile (AIBN, 1.4 wt %) was used as the initiator. The samples were sonicated for 4 minutes and polymerized for 20 hours at 70°C. The solids content of the latex dispersions was 20 wt %. The  $T_g$  according to the Fox equation (employing the literature values of  $T_g = 105^\circ\text{C}$  for PMMA and  $T_g = -54^\circ\text{C}$  for PBA) was 4°C. As  $T_g$  was below room temperature, the material film-formed easily, both in pure form and when filled with nanocellulose.

CNC dispersions with weight concentrations between 5% and 15% phase-separate into an isotropic and a chiral-nematic phase. The CNC used for printing was drawn from the

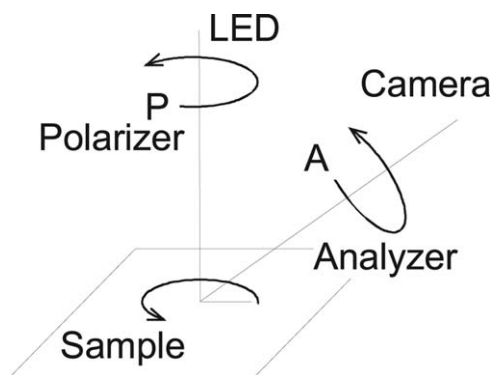


**Figure 3.** Geometry of the experiments underlying Figures 1 and 4-6.

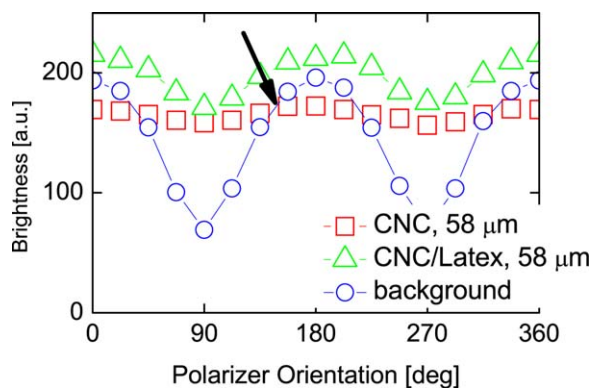


**Figure 4.** Average brightness versus angle of the polarizer ( $P$  in Figure 3). The brightness of the background is significantly reduced under crossed polarizers, while the brightness of the ink stays about the same. The arrow points to the angle, where the brightness of the background and the brightness of the areas covered with ink cross. [Color figure can be viewed in the online issue, which is available at [wileyonlinelibrary.com](http://wileyonlinelibrary.com).]

chiral-nematic fraction of such phase-separated dispersions. From the phase diagram, the solids content in this phase is known to be 15 wt %. As the dispersions were mixed at ratios of 1/1 by volume, the total solids content of the blend was 17.5 wt %. The ratio of CNC to latex was 3/4 by weight.

Spreading of the latex dispersion onto paper occurred from a pipette. On glass substrates, the material occasionally delaminates. The adhesion on paper is very good.

For comparison, samples were also prepared by spin-casting (Laurell Technologies Corporation, Model WS-650MZ-23NPP, 3000 rpm). The material used for spin-casting was drawn from the isotropic phase of a biphasic dispersion. The solids content therefore was 5 wt %.

Characterization mostly occurred as sketched in Figure 3. The sample was illuminated with a white LED (Heitronic IP44) from the top. Conventional sheet polarizers were mounted in front of the lamp and in front of the camera. The observation

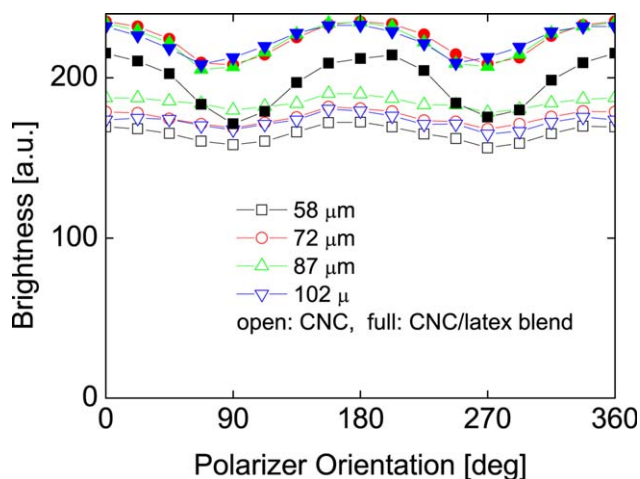


**Figure 5.** Same as Figure 4, where the average thickness of the printed layer was varied between 58 and 102  $\mu\text{m}$ . [Color figure can be viewed in the online issue, which is available at [wileyonlinelibrary.com](http://wileyonlinelibrary.com).]



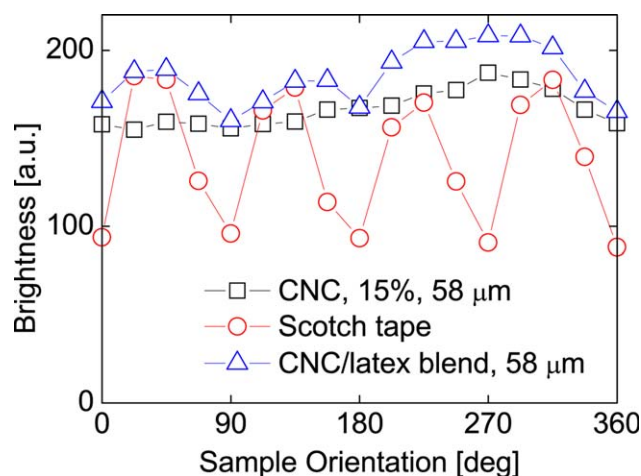


**Figure 6.** Average brightness versus orientation of the sample ( $\varphi$  in Figure 3). The brightness of the areas covered with ink only weakly depends on the orientation of the sample. This contrasts to the areas covered with Scotch tape. These vary strongly in brightness because scotch tape is birefringent with a uniform orientation of the principal axes. [Color figure can be viewed in the online issue, which is available at [wileyonlinelibrary.com](http://wileyonlinelibrary.com).]

angle of the camera was  $45^\circ$ . The microscopic texture was studied by optical microscopy (Zeiss Axioplan) and by confocal laser scanning microscopy (DM IRBE Leica Microsystems).

The contrast inversion observed upon rotating the polarizer (cf. Figure 1) was quantified on samples, which were applied as straight lines (rather than letters). Application occurred with a pipette. In order to obtain a well-defined average thickness, the area of application was limited with Scotch tape. For the comparison of the brightness between the different orientations of the polarizers, the auto-gain function of the camera was switched off. Brightness is reported in arbitrary units. The brightness was averaged over a square millimeter in the center of the sample.

## RESULTS AND DISCUSSION

### Polarization Effects in Diffuse Reflection

Figure 4 shows the brightness versus the angle of the polarizer for samples with an average thickness of  $60 \mu\text{m}$ . Squares correspond to the pure nanocellulose, upper triangles correspond to the mixture with the latex. The analyzer (in front of the camera) was in s-position, that is, the electric field vector was perpendicular to the plane of incidence. Polarizer angles of  $0^\circ$  and  $180^\circ$  denote an E-vector, which is perpendicular to the plane of incidence as defined by the position of the camera. The (dark) background clearly shows the effects of crossing polarizers. The brightness is reduced compared to parallel polarizers by about a factor of 2–3. This contrasts to the variation of brightness inside the areas coated with the ink. In these areas, the angle dependence is much reduced. Note that such a weak dependence of the brightness on the angle of the polarizer can also be achieved with conventional white ink. However, white ink at the same time is much brighter than the background. One cannot achieve contrast inversion. The anisotropic ink by itself scatters light only weakly. Its effect is based on the scrambling of polarization

of light *passing through it*. For that reason, areas coated with pure nanocellulose appear *darker* than the background when viewed with parallel polarizers. The ink redistributes the light between the two polarizations. Unfortunately, the effect is slightly weaker with the CNC/latex blend than with pure CNC.

Pure CNC is not a practical ink because it is not waterproof. The ink made from CNC alone dissolves when soaked in water. The CNC/latex blend, on the contrary, is stable in water over extended periods of time. There is no contrast inversion with the CNC/latex blend, but the ink's peculiar behavior still is easily recognized.

Figure 5 addresses the thickness dependence. Clearly, thickness is of little influence in the thickness range from  $60$  to  $100 \mu\text{m}$ . The overall brightness is somewhat larger when the average thickness is increased, but this effect has to be weighed against other properties like durability or cost.

### In-Plane Orientation

So far, the discussion focused on the orientation of the polarizers. One might hope that the orientation of the sample (the angle  $\varphi$  in Figure 3) might lead to equally impressive results. However, this is not the case as demonstrated in Figure 6. Optical observation does reveal a slight variability of the sample's appearance upon rotation in the plane of the substrate, but this variability does not translate to a significant variability after averaging over area. Clearly, the material is not well aligned.

There are two sources of poor alignment. The first is the “coffee-stain” effect, which aligns the material *after* deposition, that is, while it dries.<sup>23</sup> Immediately after deposition, one does observe an alignment along the direction of drawing. However this alignment is largely destroyed by the flow of water towards the edge of the drop. The matter has been extensively discussed in the context of latex films.<sup>24</sup> Importantly, a flow of liquid relative to a soft network of CNC rods orients the rods. The images suggest that the rods are lined up parallel to the edge. This can be explained with the compression of a loose network of rods under a viscous stress as sketched in Figure 7. A second source of misalignment can be a rough substrate (such as paper). Figure 8 demonstrates the effect. The letters were written onto a slightly translucent paper (sandwich paper, purchased at a supermarket); the images were acquired in transmission with crossed polarizers. Panel A shows the sample immediately after application of the ink. There is some birefringence; the letters are clearly distinguished from the background. The birefringence is larger for a letter written with pure nanocellulose than for the letter written with the CNC/latex blend (to the right and to the left, respectively). However, the orientation is lost after drying (panel B). If paper is the substrate, it will always be difficult to maintain a well-defined orientation after drying.

### Microscopic Texture

CNC ink displays a texture on the level of a few microns. The texture is characteristic and it can therefore serve for authentication purposes. Of course a microscope (or at least a magnifying glass) is needed. The texture of the ink produced from pure nanocellulose [Figure 9(A)] reflects the material's chiral-nematic

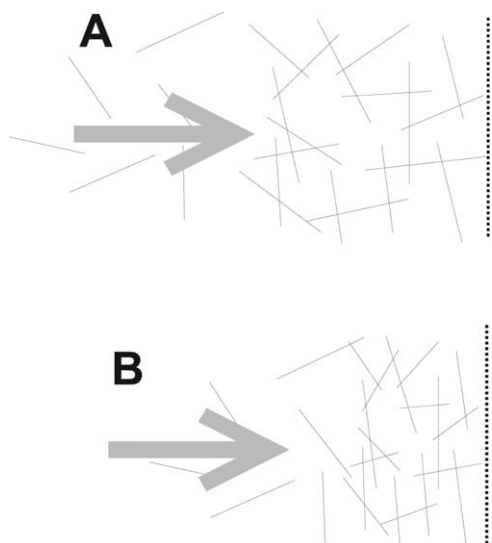


**Figure 7.** Sketch of how the coffee stain effect orients a loose network of rods at the edge of a drying droplet. The orientation is the consequence of a uniaxial compression. The dotted line is the edge of the sample. The grey arrows denote a flow of liquid towards the edge, caused by the coffee-stain effect. The flow compresses the network of nanorods.

behavior. An experienced observer recognizes the texture, although quantification and automated recognition is difficult.

The microscopic texture of the CNC/latex blend is different. It does show streaks along the preferred direction, but these are not caused by chirality. They are not related to a pitch of a twisted structure, but rather go back to demixing between polymer and cellulose on the microscale during drying. Demixing was proven with confocal microscopy. The ink was stained with a water soluble dye, namely sulforhodamine G. A variability in brightness reflects variability in concentration of the dye, rather

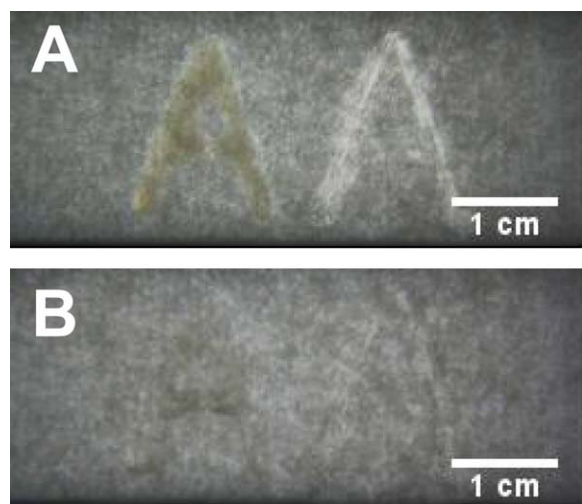


**Figure 8.** The letter “A” was written onto slightly translucent paper and imaged in transmission with crossed polarizers. Left: CNC/latex blend, Right: pure CNC. In the wet state (A) there is birefringence, which, however, is lost during drying (B). The ink applied to a rough surface is not easily aligned on the macroscopic scale. [Color figure can be viewed in the online issue, which is available at [wileyonlinelibrary.com](http://wileyonlinelibrary.com).]

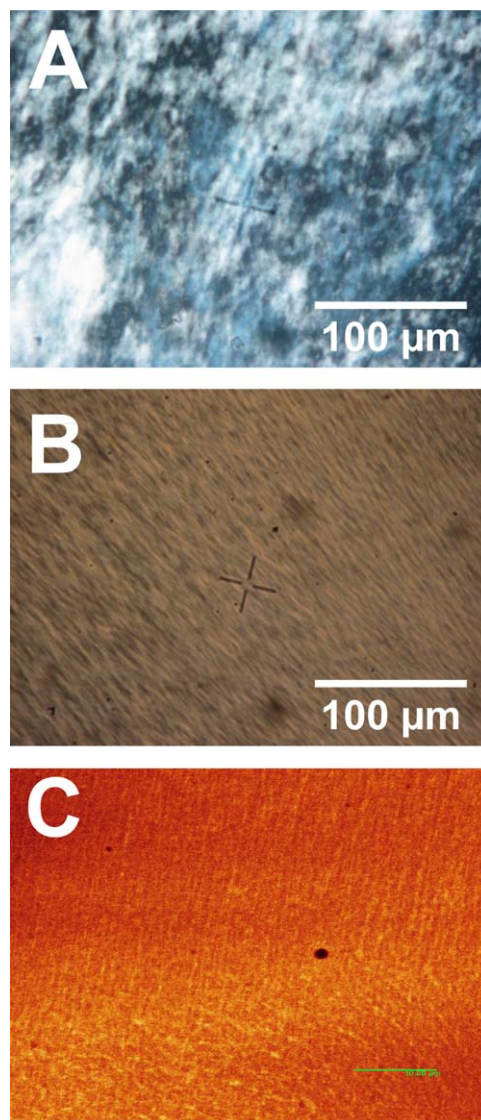


**Figure 9.** (A) Micrographs taken of a layer of pure nanocellulose, and (B) a layer of a nanocellulose/latex blend. Panel C shows image of a nanocellulose/latex blend taken with a confocal microscope. For the image in C, the CNC had been stained with sulforhodamine G. The patterns correspond to concentration fluctuations of the dye. The dry material shows [Color figure can be viewed in the online issue, which is available at [wileyonlinelibrary.com](http://wileyonlinelibrary.com).]

than orientation. As sulforhodamine G is hydrophilic, it is enriched in hydrophilic domains (the domains rich in CNC) upon microphase-separation. The pattern seen in Figure 9(B) presumably is caused by a micro-scale demixing between polymer and nanocellulose.

## CONCLUSIONS

We propose the use of a CNC latex blend as an ink for security printing. The inks are recognized as being special in diffuse reflection, if polarizers are inserted between the light source and the paper and, also, between the paper and the observer. Such devices are easily realized; their application is trivial.

Ink made of CNC appears peculiar because it scrambles the polarization from the background without being a strong scatterer, itself. Application requires a dark background. Applied to black paper, the contrast strongly depends on whether the printed area is viewed with polarizers being parallel or with crossed polarizers.

#### ACKNOWLEDGMENTS

We thank Arne Langhoff for technical help with the confocal laser scanning microscopy. Chakkresit Chindawong received a graduate fellowship from the Thai Ministry of Science and Technology.

#### REFERENCES

1. <http://prado.consilium.europa.eu/en/glossarypopup.html>, downloaded on 21.12.2013.
2. Barbera-Guillem, E. Fluorescent ink compositions comprising functionalized fluorescent nanocrystals. *US 8241765 B2* **2012**.
3. Lee, H. S.; Shim, T. S.; Hwang, H.; Yang, S. M.; Kim, S. H. *Chem. Mater.* **2013**, *25*, 2684.
4. Berne, B. J.; Pecora, R. *Dynamic Light Scattering: With Applications to Chemistry, Biology, and Physics*; Dover: New York, **2003**.
5. Ranby, B. G. *Discuss. Faraday Soc.* **1951**, *11*, 158.
6. Samir, M.; Alloin, F.; Dufresne, A. *Biomacromolecules* **2005**, *6*, 612.
7. Dufresne, A., *Nanocellulose: From Nature to High Performance Tailored Materials*; De Gruyter: Berlin, 2012.
8. Klemm, D.; Schumann, D.; Kramer, F.; Hessler, N.; Hornung, M.; Schmauder, H. P.; Marsch, S. Nanocelluloses as innovative polymers in research and application. In *Polysaccharides II, Advances in Polymer Science*; Springer Verlag, **2006**, Vol. 205, pp 49.
9. <http://umaine.edu/pdc/cellulose-nano-crystals/>, downloaded on 21.12.2013.
10. Araki, J.; Wada, M.; Kuga, S.; Okano, T. *Langmuir* **2000**, *16*, 2413.
11. Edgar, C. D.; Gray, D. G. *Cellulose* **2003**, *10*, 299.
12. Roman, M.; Navarro, F., Deposition of Cellulose Nanocrystals by Inkjet Printing. In *ACS Symposium Series, American Chemical Society: 2009*, Vol. 1019.
13. Reising, A. B.; Moon, R. J.; Youngblood, J. P. *J. Sci. Technol. Forest Prod. Process.* **2012**, *2*, 32.
14. Diaz, J. A.; Wu, X. W.; Martini, A.; Youngblood, J. P.; Moon, R. J. *Biomacromolecules* **2013**, *14*, 2900.
15. Picard, G.; Simon, D.; Kadiri, Y.; LeBreux, J. D.; Ghosayel, F. *Langmuir* **2012**, *28*, 14799.
16. Revol, J. F.; Godbout, J. D. L.; Gray, D. G. Solidified liquid crystals of cellulose with optically variable properties. *Patent 1995*, WO9521901.
17. Zhang, Y. P., Anti-counterfeiting method using synthesized Nanocrystalline Cellulose Taggants. *Ph.D. Thesis, Department of Electrical and Computer Engineering, McGill University, Montreal* **2012**.
18. Beck, S.; Bouchard, J.; Berry, R. *Biomacromolecules* **2011**, *12*, 167.
19. Favier, V.; Canova, G. R.; Cavaille, J. Y.; Chanzy, H.; Dufresne, A.; Gauthier, C. *Polym. Adv. Technol.* **1995**, *6*, 351.
20. Ben Mabrouk, A.; Vilar, M. R.; Magnin, A.; Belgacem, M. N.; Boufi, S. *J Colloid Interf. Sci.* **2011**, *363*, 129.
21. Hajji, P.; Cavaille, J. Y.; Favier, V.; Gauthier, C.; Vigier, G. *Polym. Compos.* **1996**, *17*, 612.
22. <http://umaine.edu/pdc/nanofiber-r-d/>, downloaded on 21.12.2013.
23. Deegan, R. D.; Bakajin, O.; Dupont, T. F.; Huber, G.; Nagel, S. R.; Witten, T. A. *Nature* **1997**, *389*, 827.
24. Routh, A. F. Drying of thin colloidal films. *Reports on Progress in Physics* **2013**, *76*, 046603.